Pharmaceutical Research, Vol. 25, No. 12, December 2008 (© 2008)
DOI: 10.1007/s11095-008-9692-2

Research Paper

Preparation of BMP-2 Containing Bovine Serum Albumin (BSA) Nanoparticles Stabilized by Polymer Coating

Guilin Wang,[1] Kevin Siggers,[1] Sufeng Zhang,[1] Hongxing Jiang,[2] Zhenghe Xu,[1] Ronald F. Zernicke,[3] John Matyas,[4] and Hasan Uludağ[1,5,6,7]

Received May 6, 2008; accepted July 17, 2008; published online August 15, 2008

Purpose. The purpose of this study was to investigate the preparation process of bone morphogenetic protein-2 (BMP-2) containing bovine serum albumin (BSA) nanoparticles (NPs), and to assess the bioactivity of BMP-2 encapsulated in such NPs.
Methods. The NPs were prepared by a coacervation method, and the effects of process parameters on NP size and polydispersity were examined. Polymer coated NPs were characterized with respect to amount of adsorbed polymer, particle size and zeta potential. Using bone marrow stromal cells (BMSC), biocompatibility of the NPs was investigated by the 3-(4,5-dimethylthiazol-2-yl)-2,5-diphenyl-tetrazolium bromide (MTT) Assay, and bioactivity of the encapsulated BMP-2 was investigated by alkaline phosphatase (ALP) induction and calcification.
Results. The size of NPs could be controlled in the 50–400 nm range by process parameters including BSA concentration, non-solvent:solvent ratio and pH value. After coating with cationic polymers, the particle size and zeta potential were significantly increased. MTT assay indicated no toxicity of both the uncoated and coated NPs on BMSC. Based on ALP induction and calcification, full retention of BMP-2 bioactivity was retained in the polymer-coated NPs.
Conclusions. This study described a preparation procedure for BSA NPs with controllable particle size, and such polymer-coated BSA NPs are promising delivery agents for local and systemic administration of BMP-2 in bone regeneration.

KEY WORDS: bone morphogenetic protein-2; bovine serum albumin; coacervation method; nanoparticles; polymer coating.

INTRODUCTION

Several peptides and proteins are being currently developed as potential therapeutic agents for musculoskeletal diseases. However, fundamental shortcomings have hampered their extensive clinical utility, including a relatively short half-life after administration and lack of long-term stability in physiological milieu (1). Nanoparticles (NPs) derived from biocompatible materials can serve as controlled delivery systems for therapeutic agents and help to alleviate the shortcomings of therapeutic delivery of these agents. By encapsulating a therapeutic agent, NPs isolate the agent from the physiological milieu, protect the peptide/protein drugs from enzymatic degradation, and provide a means for sustained release. A prolonged retention of biological activity is the expected outcome when therapeutic agents are delivered as a result of formulation in NPs.

The physicochemical properties of NPs are expected to be critical in controlling the release of therapeutic agents as well as the fate of the delivery systems in the body. Size and surface charge are two basic properties that can influence the biodistribution of NPs upon administration (2–5), especially after systemic injection. With respect to particle size, larger particles are more rapidly removed from the circulation by the reticuloendothelial system, and accumulate in liver and spleen at a higher extent than the smaller particles (5–7). The particles are also expected to be small enough to escape from the vascular system *via* fenestrations or cavities in the lining of the blood vessels (3). It has been suggested that the size of a solid particle should not exceed 200 nm for long-circulation (5). With respect to surface charge, small neutral particles have a longer circulation time than their anionic counterparts (8). Particles with positive surface charge is considered

[1] Department of Chemical and Materials Engineering, Faculty of Engineering, University of Alberta, Edmonton, Alberta T6G 2G6, Canada.
[2] Department of Surgery, Faculty of Medicine and Dentistry, University of Alberta, Edmonton, Alberta T6G 2G6, Canada.
[3] Departments of Orthopaedic Surgery and Biomedical Engineering, University of Michigan, Ann Arbor, MI, USA.
[4] Department of Cell Biology and Anatomy, Faculty of Medicine, University of Calgary, Calgary, Alberta, Canada.
[5] Faculty of Pharmacy and Pharmaceutical Sciences, University of Alberta, Edmonton, Alberta T6G 2G6, Canada.
[6] Department of Biomedical Engineering, Faculty of Medicine and Dentistry, University of Alberta, Edmonton, Alberta T6G 2G6, Canada.
[7] To whom correspondence should be addressed. (e-mail: hasan.uludag@ualberta.ca)

0724-8741/08/1200-2896/0 © 2008 Springer Science + Business Media, LLC

beneficial for penetrating plasma membrane of cells (9); however, it is a major disadvantage for systemic administration since cationic particles can nonspecifically bind to cell surfaces and activate the complement system (10). These adverse effects for the use of cationic particles *in vivo* can be overcome by reducing particle size and lowering surface charge (4).

Bovine serum albumin (BSA) is a naturally-occurring biomaterial that has been used as a matrix in NP preparations. Due to its proteinous nature, BSA NPs are naturally biodegradable and non-toxic (11, 12), since they can be metabolized with natural mechanisms into harmless end-products. BSA NPs can be easily prepared under mild conditions by simple coacervation, or desolvation process and their size distribution can be engineered by controlling the process parameter (2, 13–15). To obtain stable particles, glutaraldehyde (GA) was typically used to cross-link the NPs *via* the free amines after coacervation. However, the toxicity of GA is a concern for *in vivo* delivery (16, 17). GA might be also reactive with any amines of the encapsulated peptide/protein drugs (18, 19), as well as small drugs such as doxorubicin (20), which could adversely affect their integrity and bioactivity. As an alternative to GA cross-linking, we recently proposed the cationic polymers polyethylenimine (PEI) to stabilize BSA NPs. This method was used in our lab to encapsulate bone morphogenetic protein-2 (BMP-2) during BSA NP preparation by coacervation method (21). A high loading efficiency (>90%) and controlled release of bioactive BMP-2 from the PEI-coated BSA NPs were achieved. However, the BSA NPs used in that study were prepared by using ethanol as the non-solvent, which led to relatively large NPs (230–400 nm) especially after PEI coating. The NPs coated with higher concentrations of PEI (>0.1 mg/mL) also indicated some toxicity as compared to the uncoated NPs.

The present study was conducted to better understand the process parameters that control NP size. The effects of such process parameters as BSA concentration, pH value, non-solvent/water ratio and stirring rate on NP size and polydispersity were investigated. The feasibility of coating NPs with an additional cationic polymer, poly-L-Lysine (PLL), was explored at relatively low concentrations (<0.1 mg/mL). Our results identified several process parameters that significantly affected the NP size, and indicated PLL to be a suitable substitute for PEI. The final particle size obtained in this study typically ranged between 200–400 nm after polymer coating, and retained the bioactivity of BMP-2 with no obvious cytotoxicity to bone marrow stromal cells (BMSC).

MATERIALS AND METHODS

Materials

BSA, 3-(4,5-dimethylthiazol-2-yl)-2,5-diphenyl-tetrazolium bromide (MTT), *p*-nitrophenol phosphate, ascorbic acid, β-glycerolphosphate, PLL (Mw~24 kDa) and branched PEI (Mw~25 kDa) were obtained from Sigma–Aldrich (St. Louis, MO, USA). The non-solvents, ethanol and acetone, were reagent grade solvents from Fisher Scientific. Reagent-grade NaCl was from EMD Chemical Inc. (Darmstadt, Germany). Recombinant human bone morphogenetic protein-2 (BMP-2) was expressed in *Escherichia coli* and purified as described before (22). Fluorescein isothiocyanate (FITC) was obtained from Pierce (Rockford, IL, USA) and it was used to label the polymers PLL and PEI according to previously described methodology (23). Dulbecco's Modified Eagle Medium (DMEM), Hank's Balanced Salt Solution (HBSS), GlutaMax-1 (GM), penicillin (10,000 U/mL) and streptomycin (10,000 μg/mL) were from Invitrogen (Carlsbad, CA, USA). Fetal bovine serum (FBS) was from Atlanta Biologics (Atlanta, GA, USA). All tissue culture plasticware was from Corning (Corning, NY, USA). The Spectra/Por dialysis tubing with molecular weight cut-off of 12–14 kDa was acquired from Spectrum Laboratories (Rancho Dominguez, CA, USA) and used in all dialysis procedures. Distilled/deionized water (ddH_2O) used for buffer preparations were derived from a Millipore ELIX purification system. The phosphate-buffered saline (PBS; pH 7.4) used in dialysis was diluted from the stock of 10X PBS (80 g/L NaCl, 2 g/L KCl, 14.4 g/L Na_2HPO_4 and 2.4 g/L KH_2PO_4). Phosphate buffers used to dissolve the reagents were diluted from the stock prepared by mixing 0.5 M Na_2HPO_4 and 0.5 M $NaH_2PO_4.H_2O$ solutions to obtain the appropriate pH.

Preparation of BSA NPs

The BSA NPs were prepared by a coacervation method based on previously published literature (2, 13), except cross-linking by GA was eliminated as described previously (21). The non-solvents used were either ethanol or acetone. In a typical process, the non-solvents were added drop-wise to an aqueous BSA solution under constant stirring. Initially by using ethanol, the influences of BSA concentration, pH value of the aqueous solution, and ethanol/water ratio (the final volume ratio of ethanol added to the starting aqueous BSA solution) on particle size were examined independently. For this, the BSA solution at given concentration was mixed with equal volume of 10 mM NaCl or 10 mM phosphate buffers of pH 4.3, 5.5, 7.4 and 9.3, and coacervated with different volumes of ethanol under constant stirring (800 rpm). A systematic method, Taguchi Method (TM) with an orthogonal array design (24, 25), was next applied to re-analyze the effects of the process parameters. The experimental control factors and their levels selected for the statistical testing are listed in Table I. From the numbers of factors and levels, the total degree of freedom (*dof*) for this system was $3\times(4-1)+(3-1)+1=12$. This *dof* value led to the choice of an L18(43×3) orthogonal array. The control factor levels for the testing were arranged in the orthogonal array as shown in Table II. Then, ethanol was replaced by acetone as the non-solvent to investigate the dependence of the particle size on the non-

Table I. Experimental Control Factors and their Levels for the Statistical Experiment Testing

	Factors	Level 1	Level 2	Level 3	Level 4
A	BSA concentration (mg/mL)	10	20	30	50
B	Ethanol:water ratio	1	2	4	6
C	pH value	4.3	5.5	7.4	9.3
D	Stirring rate (rpm)	400	800	1200	

Table II. Orthogonal Array and Results of the Statistical Experiment Testing

	A	B	C	D	Results			
Experiment no.	[BSA] (mg/mL)	Ethanol:water ratio	pH value	Stirring rate (rpm)	Size (nm)	SD (nm)	PDI	SD
1	10	1	4.3	400	334.2	11.5	0.286	0.236
2	10	2	5.5	800	241.8	9.6	0.235	0.056
3	10	4	7.4	1200	128.9	9.0	0.263	0.155
4	10	6	9.3	400	122.2	37.0	0.677	0.284
5	20	1	5.5	800	186.5	5.1	0.506	0.013
6	20	2	4.3	1200	296.8	4.2	0.161	0.027
7	20	4	9.3	400	158.0	1.9	0.117	0.043
8	20	6	7.4	800	97.6	0.6	0.097	0.015
9	30	1	7.4	1200	58.7	10.0	0.599	0.123
10	30	2	9.3	1200	102.9	4.6	0.636	0.054
11	30	4	4.3	800	260.6	0.8	0.256	0.058
12	30	6	5.5	400	163.7	2.3	0.161	0.019
13	50	1	9.3	800	93.0	2.6	0.509	0.015
14	50	2	7.4	400	149.0	5.7	0.454	0.069
15	50	4	5.5	1200	137.8	4.7	0.593	0.031
16	50	6	4.3	1200	193.1	1.7	0.285	0.01
17	30	4	9.3	800	150.4	0.8	0.188	0.065
18	20	6	7.4	400	92.8	3.2	0.377	0.098

Data were expressed as mean and SD (n=3). PDI=polydispersity index

solvent. In all cases, the desolvated mixtures were stirred for 3 h after addition of non-solvent, and stored at 4°C for particle size characterization and polymer coating.

Polymer Adsorption to NPs

Investigation of polymer adsorption to NPs were carried out by using NPs prepared from 10 mg/mL BSA in 10 mM phosphate buffer (pH 7.4) and with acetone:water ratio of 4. Three hundred microliter of NPs dispersion (with acetone) was added to equal volumes of 0, 10, 20, 50 and 100 μg/mL PLL or PEI in 10 mM phosphate buffer solution (pH 7.4). The adsorption process was allowed for 1 h at room temperature and under constant shaking at 500 rpm. The coated NPs were then cleaned from the acetone and non-adsorbed polymer by extensive dialysis against 1 mM NaCl (×3). In some experiments, FITC-labeled polymers were used for NP coating in order to determine the exact amount of polymers adsorbed to the NPs (milligram per gram BSA). As above, the FITC-PLL or FITC-PEI coated NPs were dialyzed against 1 mM NaCl (×3) to remove the acetone and excess polymer. Two hundred microliters of the samples in duplicate was then added to a black 96-well plate (NUNC, Rochester, NY, USA) and the fluorescence (λ_{ex}=485 nm; λ_{em}=527 nm) was determined with a multiwell plate reader (Thermo Labsystems, Franklin, MA, USA). The amounts of PLL-FITC or PEI-FITC adsorbed on the BSA NPs were calculated based on calibration curves generated by using known concentrations of PLL-FITC or PEI-FITC in 1 mM NaCl.

Hydrodynamic Size and Zeta Potential of NPs

The mean particle size and polydispersity index of polymer-coated and uncoated NPs were determined by photon correlation spectroscopy using a Malvern Zetasizer 3000HS (Malvern Instruments Ltd., UK). The measurements were carried out at 25°C using a 633 nm He–Ne laser at a scattering angle of 90°. The NPs without coating were directly

Table III. Data Analysis of the Statistical Experiment Testing

	Particle size (nm)				PDI			
Analysis	A	B	C	D	A	B	C	D
K_1	827.1	672.4	1084.7	1019.9	1.461	1.900	0.988	2.072
K_2	935.4	790.5	610.2	991.0	1.857	1.486	1.495	1.791
K_3	734.9	835.7	527.0	918.2	1.840	1.417	1.790	2.537
K_4	572.9	669.4	626.5		1.841	1.597	2.127	
k_5	206.8	168.1	271.2	170.0	0.365	0.475	0.247	0.345
k_2	187.1	197.6	152.6	165.2	0.371	0.372	0.374	0.299
k_3	147.0	167.1	105.4	153.0	0.368	0.283	0.358	0.423
k_4	143.2	133.9	125.3		0.460	0.319	0.425	
R	63.6	63.7	165.8	17.0	0.095	0.192	0.178	0.124

Level total K_i and level average k_i were the sum and average of the results of those experiments which had the ith level of a given factor. R was the maximum variance ($\max\{k_i\}$–$\min\{k_i\}$) of each factor. For example: K_1(A)=334.2+241.8+128.9+122.2=827.1 (nm), k_1(A)=K_1(A)/4=206.8 (nm), R(A)=206.8–143.2=63.6 (nm)

used for measurement in the coacervation system with ethanol or acetone. The polymer-coated NPs obtained after dialysis were diluted 1:5 with 1 mM NaCl before the measurement. The particle size values for each type of NPs were derived from at least three measurements in each batch, and the final values indicated were an average of three independent batches of NP preparations.

The surface charge of the polymer-coated BSA NPs was investigated by measuring the electrophoretic mobility of the particles using the Malvern Zetasizer 3000HS at 25°C. The conversion to zeta potentials was performed using Smoluchowsky relation $\zeta = u \cdot \eta / \varepsilon_0 \varepsilon_r$, where u is the electrophoretic mobility, ε_0 and ε_r are the permittivity of the vacuum and the relative permittivity of the medium respectively, η is the viscosity of the medium and ζ is the zeta potential. The coated samples for zeta potential measurement were prepared after dialysis and diluted 1:5 in 1 mM NaCl solution. The reported zeta potentials of the NPs were derived from three independent batches of NP preparations.

Atomic Force Microscopy

The morphology of the uncoated and coated BSA NPs was examined by MFP-3D atomic force microscopy (AFM; Asylum Research, Santa Barbara, CA, USA) using AC240TS cantilever throughout all measurements. The NP samples were appropriately diluted to visualize individual particles and 5 μL of the diluted sample was dropped onto the surface of PELCO^R Mica Discs (TED PELLA, Inc.; Redding, CA, USA), and observed after drying under room temperature. Images were processed and analyzed by the Igor Pro imaging software (version 5.04 B).

Encapsulation of BMP-2 in BSA NPs

A 10 mg/mL BSA solution (180 μL) was mixed with equal volume of 10 mM phosphate buffer of pH 7.4 in a glass vessel. After stirring for 15 min, 90 μL of 0.5 mg/mL BMP-2 was added to this solution. After incubation for 1 h, the aqueous solution was desolvated with dropwise addition of acetone (acetone/water ratio—4), and then stirred for 3 h at 800 rpm at room temperature. The BMP-2 loaded NPs were coated with PLL and PEI (50 μg/mL) as in previously described procedure. For comparison, BSA NPs without BMP-2 were used for coating under similar conditions. After the polymer adsorption, the coated NPs were dialyzed against PBS (×2), and then against low-glucose DMEM with 1% antibiotics (for hBMSC) or high-glucose DMEM with 100 μg/mL streptomycin and 100 U/mL penicillin (for rBMSC). All solutions/apparatus used for BMP-2 encapsulation were sterilized before use, and procedures were performed in a biological safety cabinet to maintain sterility.

Biocompatibility of NP Formulations

Two types of cells, human and rat bone marrow stromal cells (hBMSC and rBMSC respectively) were used for assessment of NP biocompatibility. The preparation of hBMSC and rBMSC were described in (26) and (22), respectively. Both cells were cultured in an osteogenic medium, where the basal medium was supplemented with 50 μg/mL ascorbic acid, 100 nM dexamethasone and 5 mM β-glycerolphosphate. In the case of hBMSC, the basal medium was low-glucose DMEM containing 10% FBS, 0.7% GM, 100 μg/mL streptomycin, 100 U/mL penicillin, whereas in the case of rBMSC, the basal medium was high-glucose DMEM, 10% FBS, 100 μg/mL streptomycin and 100 U/mL penicillin. The NPs were prepared as described above and coated with PEI and PLL (10, 20, 50 and 100 μg/mL). The final dialysis of the NPs was preformed against low-glucose DMEM (for hBMSC) containing 1% antibiotics or high-glucose DMEM (for rBMSC) containing 100 μg/mL streptomycin and 100 U/mL penicillin. An aliquot of NP dispersion was then incubated with the cells (in triplicate) grown in 24-well tissue culture plates. After a 48 h incubation period in a humidified atmosphere with 95/5% air/CO2, 200 μl of the MTT solution (5 mg/mL in HBSS) was added to the 1.0 mL culture medium in each well. The cells were incubated for a further 2 h, the supernatant was removed, and 1.0 mL of DMSO was added to the cells to dissolve the formazan crystals formed. The optical density of the solution was measured by a multi-well plate reader at 570 nm. Uncoated BSA particles and untreated cells served as controls.

BMP-2 Bioactivity by ALP assay

A kinetic alkaline phosphatase (ALP) assay was used to determine the bioactivity of BMP-2 encapsulated in the PEI- and PLL-coated (50 μg/mL) and uncoated BSA particles. For comparison, the ALP assay was performed on similar NPs without BMP-2. Following NP fabrication, all particles were dialyzed in the same manner as described in the MTT procedure. hBMSC and rBMSC were incubated (in triplicate) with the NPs at the estimated concentration of 1 μg/mL of BMP-2 per well in 24-well plates (1 mL medium/well). The cells were incubated with the NPs for 3, 7 and 14 days. The medium was not changed in the case of 3 and 7 day incubation, but 1 mL of fresh medium was added to the cells after 7 days in the case of 14 day incubation. To perform the ALP assay, the cells were washed with an HBSS solution (×2) and lysed with 400 μL ALP buffer (0.5 M 2-amino-2-methylpropan-1-ol and 0.1% (*v*/*v*) Triton-X; pH=10.5). After 1.5 h, 200 μL of 1.0 mg/mL ALP substrate (*p*-nitrophenol phosphate) was added to 200 μL of the cell lysate, and the rate of change in the optical density was determined with an enzyme-linked immunosorbent assay (ELISA) plate reader by measuring the absorbance (405 nm) at intervals of 90 s for 8 cycles. Untreated cells and cells treated with 1 μg/mL of free BMP-2 served as negative and positive controls, respectively. A standard curve based on known concentration of *p*-nitrophenol in ALP buffer was used to convert the absorbance values obtained into concentration of *p*-nitrophenol formed per minute.

Calcification Assay

A calcification assay was used to measure the amount of calcium formed on the samples following the ALP assay. Only rBMSC was used in this study, since hBMSC did not provide calcification during the 14-day time period used in this study. After the removal of the lysed cells for ALP assay, 0.5 mL of 0.5 M HCl was added to each well for 48 h to dissolve the calcium/phosphate deposits formed. Twenty microliters of the

dissolved calcium solution was added to 50 μL of a solution containing 0.028 M 8-hydroxyquinoline and 0.5% (*v*/*v*) sulfuric acid, as well as 0.5 mL of solution containing 3.7×10^{-4} M *o*-cresolphthalein and 1.5% (*v*/*v*) AMP (2-amino-2-methyl-propan-1-ol). The absorbance was measured with an ELISA plate reader at 570 nm. A standard curve based on known concentration of calcium standards (SIGMA) was used to convert the absorbance values obtained into concentration of calcium.

Data Analysis

All data shown in figures are summarized as mean ± SD, and where indicated, statistical differences ($p<0.05$) between group means were analyzed by the two-sided Student's *t*-test or by analysis of variance.

RESULTS AND DISCUSSION

Effect of Coacervation Process Parameters on NP Properties

In order to understand factors affecting the properties of NP prepared from the coacervation procedure, series of experiments were performed by controlling the BSA concentration (Fig. 1A, B), the pH of coacervation medium (Fig. 1 C, D) and the non-solvent/water ratio during NP formation (Fig. 1E, F). To explore the effect of protein concentration, BSA solutions prepared at 10, 20, 30 and 50 mg/mL were mixed with 10 mM NaCl, and coacervated with ethanol:water ratios of 1, 2, 4 and 6. The BSA concentration significantly influenced the size of the resultant NPs. As shown in Fig. 1A, a gradual reduction in NP size was observed as the BSA concentration was increased from 10 to 50 mg/mL. This was the case for all ethanol/water

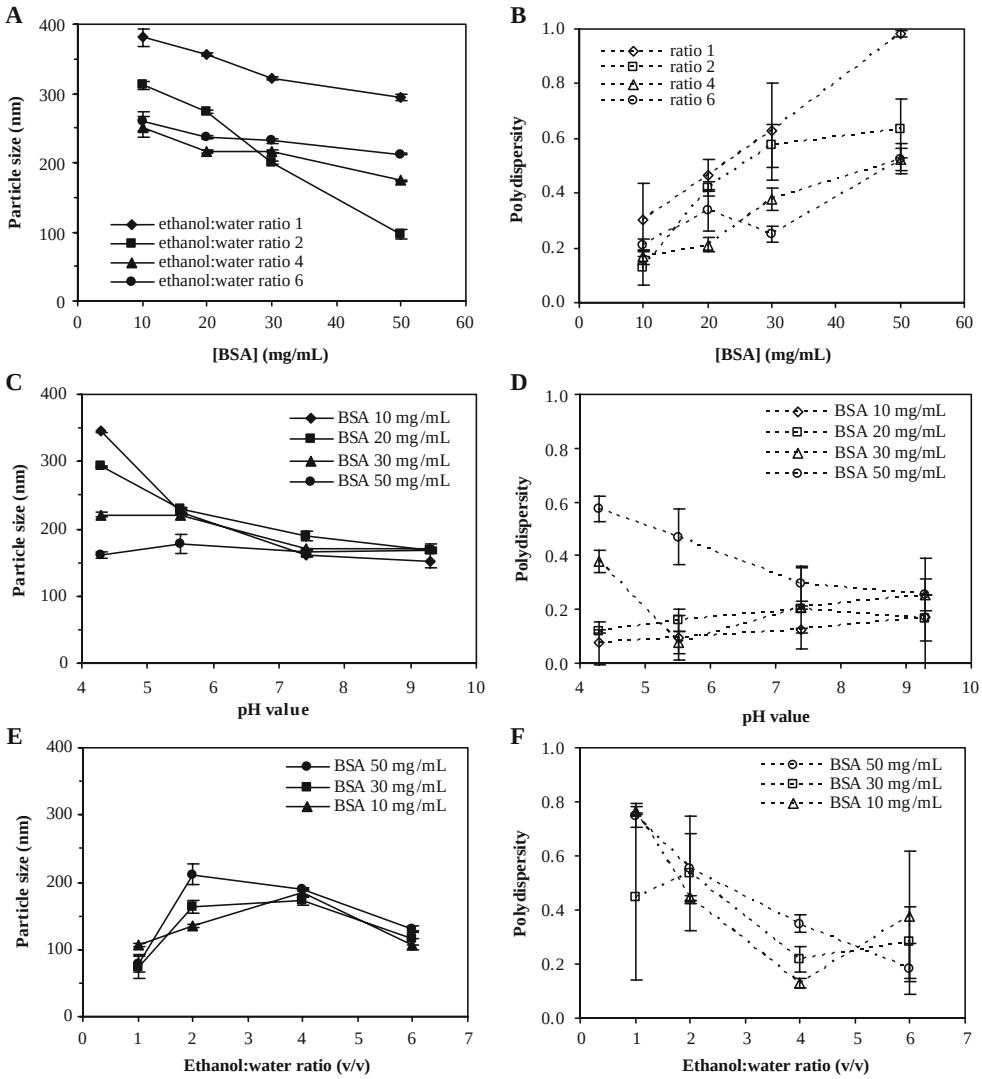

Fig. 1. Influence of BSA concentration (**A**, **B**), pH value of coacervation solution (**C**, **D**) and ethanol/water ratio (**E**, **F**) on particle size and polydispersity of BSA NPs. BSA concentrations shown were the initial concentration mixed with equal volume of 10 mM NaCl in (**A**) and (**B**), 10 mM phosphate buffer (pH 4.3, 5.5, 7.4 and 9.3) in (**C**) and (**D**) with ethanol/water ratio of 4, and 10 mM phosphate buffer (pH 9.3) in (**E**) and (**F**) before coacervation. Data were expressed as mean ± SD of three independent NP preparations ($n=3$). The sizes of NPs prepared using ethanol as the non-solvent were mostly in the 100–400 nm range. Both the particle size and polydispersity were significantly dependent on these three process parameters investigated.

ratios investigated. A gradual increase in polydispersity, however, was also observed as the BSA concentration was increased from 10 to 50 mg/mL (Fig. 1B). The results in this concentration range were consistent with the results form an earlier study by Rahimnejad *et al.* (15). Increased BSA concentration during the coacervation process presumably led to increased nucleation of BSA particles upon ethanol exposure, leading to eventual formation of smaller NPs. The uncoated NP sizes obtained from our process were typically above 100 nm, and the smallest NPs (97 nm) were obtained with BSA concentration of 50 mg/mL and ethanol ratio of 2.

The effect of coacervation medium pH on NP sizes was then explored by changing the pH of the 10 mM phosphate buffer used to form coacervates. The BSA concentrations used in this study was 10, 20, 30 and 50 mg/mL, and the pH of the aqueous medium was varied from 4.3 to 9.3. As summarized in Fig. 1C, NP size was inversely related to the pH of the medium, but the concentration of BSA also affected this behavior. As the pH of the phosphate buffer was increased from 4.3 to 9.3, a decrease in size from 350 to 150 nm was noted for the 10 mg/mL BSA. The decrease in size was drastic when the pH was lower than 7.4, but not afterwards. A similar behavior was noted for 20 and 30 mg/mL BSA concentrations. For the 50 mg/mL BSA concentration, the effect of pH on NP size was not as significant as the lower concentrations, with typical NP size obtained ~160 nm irrespective of the pH. This observation was in good agreement with the earlier work of Lin *et al.* (14) and Langer *et al.* (2), who studied the preparation of human serum albumin (HSA) NPs by ethanol and acetone induced coacervation, respectively. The decrease of NP size with increasing pH value was considered to be due to increased ionization of the BSA whose isoeletric point (pI) is 4.7. At higher pH values, BSA has a net anionic charge, which acts as repulsive force against particle aggregation. This is unlike the neutral state of BSA at the lowest pH used in our study (4.3), which gave relatively neutral BSA molecules more amenable for protein-protein interactions and, possibly aggregation. When other proteins are used in this process, the pH value of the coacervation medium might need to be adjusted depending on the pI of the employed proteins.

The effect of ethanol/water ratio on NP properties is shown in Fig. 1E (size) and Fig. 1F (polydispersity). The NP size was significantly increased up to ethanol/water ratio of 2, whereas the polydispersity decreased, which was indicative of the incomplete coacervation process with a ratio less than 2. The NP size tended to decrease as the ethanol/water ratio was increased to 6, with a corresponding reduction in polydispersity. A similar observation was reported in a previous study by Weber *et al.* (13). These observations can be explained by a basic mechanism underlying the coacervation process investigated by Kreuter (27), where gelatin was used for NP preparation. At low ethanol/water ratio (<2) before complete coacervation, the increased amount of solvated BSA in aggregates might have led to increasing particle size. At relatively higher ethanol/water ratio, where the coacervation process was completed, the decrease in particle size with increasing ethanol volume was the likely result of more solvent extraction or diffusion into the non-solvent phase, thus making the formed NPs more restrained.

Process Optimization by Taguchi Method

To optimize the NP preparation procedure, TM was applied to re-analyze the effects of the process parameters tested above. TM is a statistical method for analyzing experimental data for determining and optimizing the effects and levels of the various factors involved in a system (24, 25). As an integrated, statistical way of testing pair-wise interactions instead of varying one parameter at a time, it can create an efficient and concise test set with many fewer test cases than testing all combinations of all variables. Considering the system listed in Table I, three factors (BSA

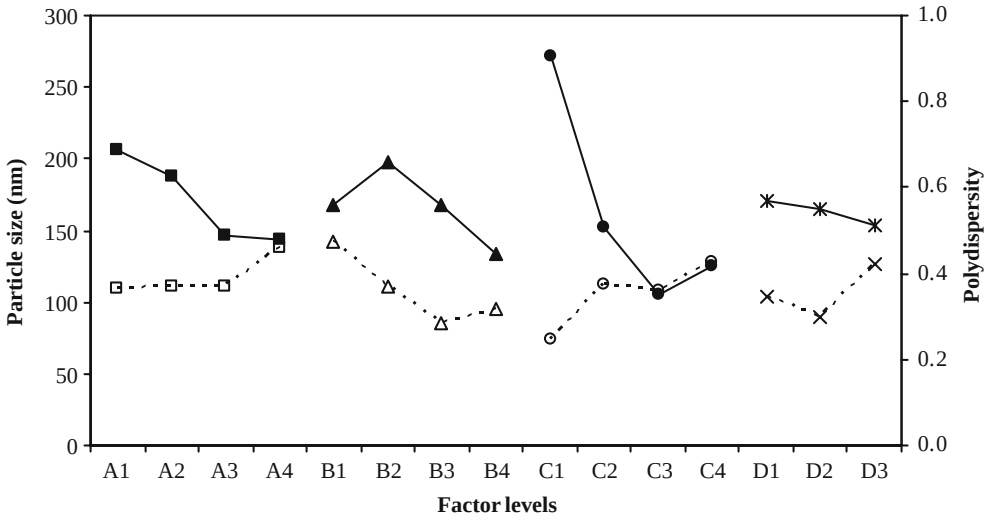

Fig. 2. Dependence of particle size (*solid symbol*) and polydispersity (*open symbol*) on *A*: BSA concentration (*square*), *B*: pH value (*triangle*), *C*: ethanol/water ratio (*circle*) and *D*: stirring rate (*cross*). The factors and levels were from Table I. Note that the effects of BSA concentration, pH of the coacervation medium, and ethanol/water ratio on NP size and polydispersity examined by the Taguchi method were consistent with the independent experiments shown in Fig. 1.

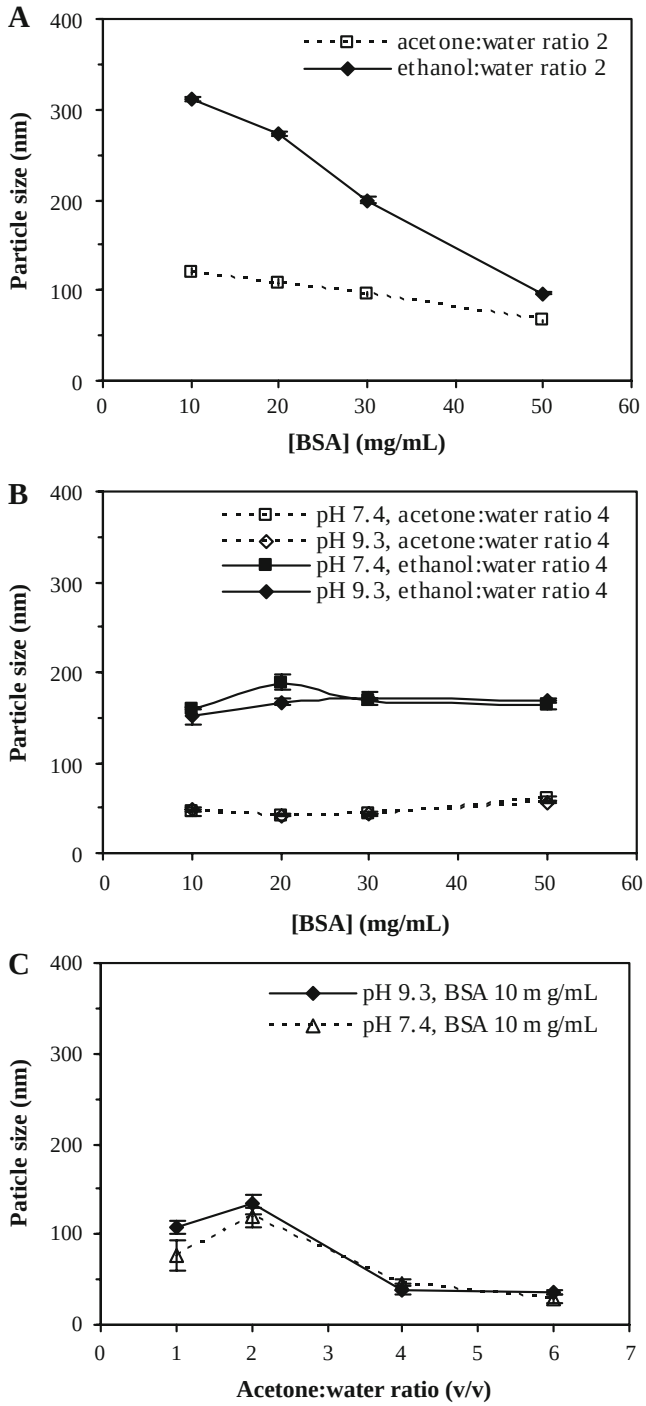

Fig. 3. Comparison of the size of BSA NPs prepared by using ethanol and acetone as the non-solvent. BSA concentrations shown were the initial concentration mixed with either 10 mM NaCl (**A**), or 10 mM phosphate buffer (**B**) with pH 7.4 and 9.3 before coacervation. Note that acetone yielded NPs with smaller sizes than ethanol under all conditions tested. (**C**) Effect of acetone/water ratio on NP size when 10 mg/mL BSA was mixed with phosphate buffer at pH 7.4 and 9.3. As compared to ethanol (see Fig. 1C), acetone also yielded smaller particles at the highest acetone/water ratio. Data in all graphs were expressed as mean ± SD of three independent NP preparations (n=3).

concentration, ethanol/water ratio, and pH value) with four values each and one factor (stirring rate) with three values were used for process optimization. The exhaustive test set would have required 192 (43×3) test cases. The test set created by TM (using the orthogonal array in Table), however, had only 18 test cases with all of the pair-wise combinations.

After running the orthogonal array with a set of experiments, the analysis of the results was constructed in Table III by the level total, level average (k_i) and the maximum variance (R) from each factor with respect to particle size and polydispersity. Comparing the k_i and considering a 'Smaller-Is-Better' principle, the optimum condition with those levels that had the smallest level averages were decided as $A_4B_4C_3D_3$ for particle size and $A_1B_3C_1D_2$ for polydispersity. Based on the R of particle size as shown in Table III (R for BSA concentration, ethanol/water ratio, pH and stirring rate were 63.6, 63.2, 162.6 and 17.0 nm, respectively), TM results indicated the order of the importance of the parameters as: pH value > ethanol/water ratio ~ BSA concentration > stirring rate. As seen from Fig. 2, the effects of BSA concentration, pH value and ethanol/water ratio on the particle size and size distribution were both consistent with the results from independent experiments shown in Fig. 1.

Acetone as a Coacervation Agent

The size of the NPs obtained in previous studies, where ethanol was used as the non-solvent, was generally greater than 100 nm. This was in line with the most studies reported in the literature, where NP sizes between 100 and 600 nm were reported (2). An exception to these observations was an early study reported by Lin *et al.* (14), where acetone was used for protein coacervation to obtain ~100 nm HSA particles. Ethanol had not been used by these investigators and it was not known if the smaller particle size was due to acetone or some other process parameter(s). To determine if

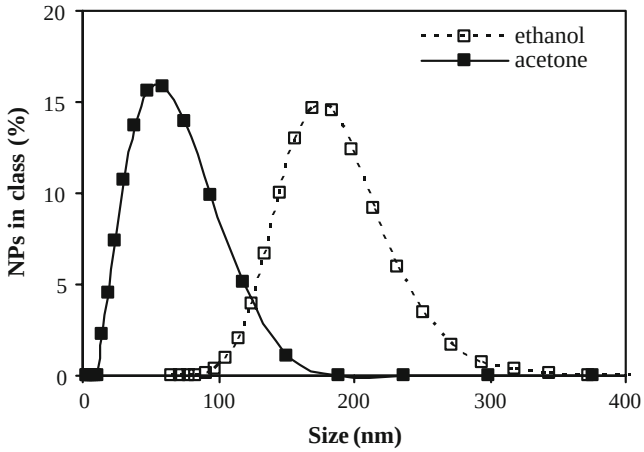

Fig. 4. Size distribution of the NPs prepared by using acetone (*solid*) and ethanol (*dashed*) as non-solvent. NPs were prepared by using 10 mg/mL BSA mixed with equal volume of 10 mM phosphate buffer of pH 7.4, followed by dropwise addition of four volumes of acetone or ethanol. The distribution was based on intensity from dynamic light scattering measurement. Note that the size range of BSA NPs prepared by using acetone was lower.

acetone substitution for ethanol could indeed lead to smaller NPs, we used our established process to prepare NPs from BSA solution dissolved in NaCl (Fig. 3A) or phosphate buffer (Fig. 3B). The use of acetone consistently gave smaller particles as compared to ethanol for all BSA concentrations tested (10–50 mg/mL). The smallest NPs (~50 nm) were obtained with BSA dissolved in phosphate buffer (pH 7.4 or 9.3) and at acetone/water ratio of 4. As with ethanol, acetone/water ratio significantly affected the size of the final NP obtained (Fig. 3C). The NP size increased from the ratio of 1 to 2, and decreased afterwards to ~50 nm at acetone/water ratios of 4–6. This trend was similar whether the pH of the medium was 7.4 or 9.3. The results from NP formation in pH of 4.3 and 5.5 were not shown since obvious precipitates were formed under such conditions, rather than suspended NPs. The typical size distributions for the ethanol and acetone desolvated NPs was illustrated in Fig. 4 (10 mg/mL BSA in 10 mM phosphate buffer of pH 7.4 with non-solvent/water ratio of 4). The distribution was skewed to the right, with a small percentage of larger NPs present in both preparations. Whereas acetone desolvated NPs had a size range of 20–150 nm, the ethanol desolvated NPs had a size range of 100–300 nm.

Collectively, these studies led us to conclude that the use of acetone for BSA desolvation led to smaller NPs as compared to NPs formed by ethanol desolvation. The reason for the smaller NPs obtained from acetone desolvation might be related to acetone being a better non-solvent for BSA than ethanol, thus creating smaller particles with sizes similar to the primary particles (~50 nm in diameter) proposed by the phase inversion theory (28). Though both ethanol and acetone are miscible with water, which is essential for the formation of particle nuclei and growth by solvent extraction, the better insolubility of BSA with the bulk non-solvent might be limiting smaller spatial expansion of the particles. Unfortunately, theoretical discussions on this issue are extremely rare at present, and thermodynamic and kinetic data are needed for further understanding of this process.

Coating of BSA NPs with PLL and PEI

BSA NPs prepared by coacervation are usually stabilized by GA crosslinking *via* the protein amines. However, as discussed above, besides potential toxicity of GA for *in vivo* use, GA cross-linking may affect the release rate and bioactivity of the encapsulated drugs. An alternative approach for NP stabilization is surface coating with a suitable molecule, for example, cationic polymers in the case of anionic BSA NPs. We previously reported the use of PEI for this purpose (21), where the surface charge of the particles shifted from negative to neutral or slightly positive. This change may reduce the plasma protein adsorption on particle surfaces and thus facilitate *in vivo* application of NPs (29, 30). We considered the well-known toxicity of PEI to be a potential shortcoming and, hence, explored another cationic polymer, PLL, for coating BSA NPs.

The BSA NPs were coated by different concentrations of PEI and PLL (10, 20, 50 and 100 μg/mL) and the amount of polymer adsorbed was quantitated by using FITC-labeled polymers. The results (milligram polymer/gram BSA) calculated from the calibration curves for individual polymers were summarized in Fig. 5A. As the coating polymer concentration

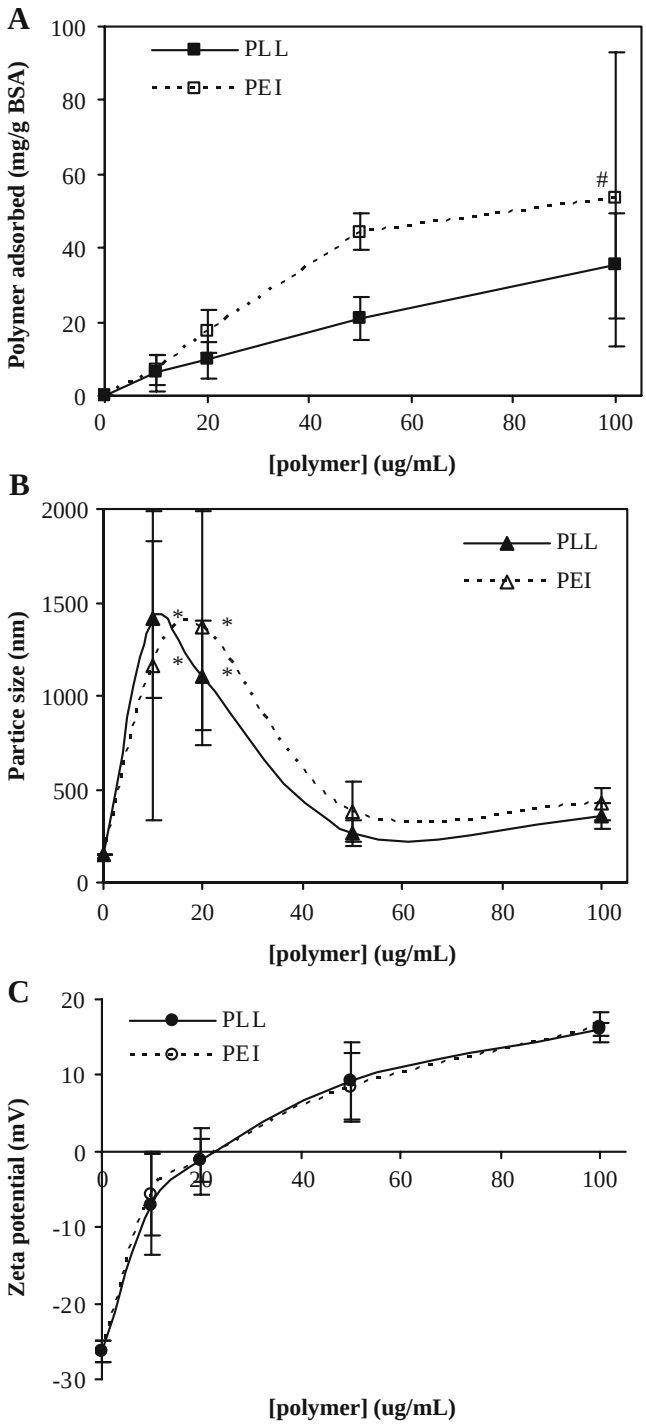

Fig. 5. The amount of polymer adsorbed onto NPs (**A**), mean particle diameter (**B**) and zeta potential (**C**) of NPs coated with different concentrations of PLL and PEI. The amounts of PEI adsorbed onto the NPs were slightly more than the PLL at concentrations higher than 20 μg/mL. Note the drastic increase in particle size at low polymer concentrations for both polymers. The zeta potential of the PLL and PEI coated NPs increased gradually from −26 mV for uncoated NPs to ~16 mV at polymer concentration of 100 μg/mL. There was slight but not significant difference between PLL and PEI coated NPs with respect to particle size and zeta potential. Data in all graphs were expressed as mean ± SD of three independent NP preparations (n=3). *Number sign*: some precipitates were observed for one sample; *asterisk*: Polydispersity greater than 0.7.

was increased, the amount of adsorbed polymer was increased as expected. There was no difference in the adsorbed polymer between PLL and PEI at 10 μg/mL, but a difference was noted at higher concentrations (significantly different at 50 μg/mL, but not at 100 μg/mL due to large SDs).

The size of the resultant NPs are summarized in Fig. 5B. The mean particle size showed a dramatic change as a function of polymer concentration: a maximal size of >1000 nm was obtained at low polymer concentrations (10–20 μg/mL), after which the size of the NPs was reduced to 200–400 nm at presumably excess polymer concentration. Coating at polymer concentration of 10 and 20 μg/mL also led to a significant variation in particle size (large SD in Fig. 5B), presumably due to a bridging flocculation among the particles leading to aggregation (31). For higher coating concentrations, the polymers presumably attained a better coating of the surfaces, with little bridging among the particles. Both PEI and PLL displayed the same behavior in this respect, given similar changes of NP size as a function of polymer concentration for both polymers.

The zeta potential of the polymer coated NPs increased gradually from −26 mV of uncoated NPs to ~16 mV as polymer concentration was increased to 100 μg/mL, as shown in Fig. 5C. For NPs coated with 10 and 20 μg/mL polymer concentrations, the surface charge of the coated particles was close to neutral, which was the likely reason for the dramatic increase in particle size in Fig. 5B. The surface charge of particles coated with 50 and 100 μg/mL polymer became increasingly positive, which might have led to repulsive forces among the particles and prevented NP aggregation. It was interesting to note that there was no significant difference between PLL and PEI coated NPs with respect to zeta potential (and size), even though the amount adsorbed onto the NPs was higher for PEI as compared to PLL. This may suggest that the PEI penetrates deeper into the particles when it is conjugated to the surface or a denser combination was formed between the PEI and BSA NPs.

The BSA NPs were analyzed by AFM to confirm the size of the particles measured. As shown in Fig. 6A, the NPs after the coacervation process were uniform in size, and generally spherical with smooth surface characteristics. No visible aggregates were evident. Figure 6B and C are typical AFM images for particles coated with 50 μg/mL PLL and PEI, respectively. Larger particles after coating were evident, and the less uniform in particle size and rough surface were seen for the coated particles. The sizes obtained from these images were typically in the range of 100–200 nm, smaller than the measurement from dynamic light scattering results, which was possibly due to the shrinkage of the particles during the drying process for the AFM imaging.

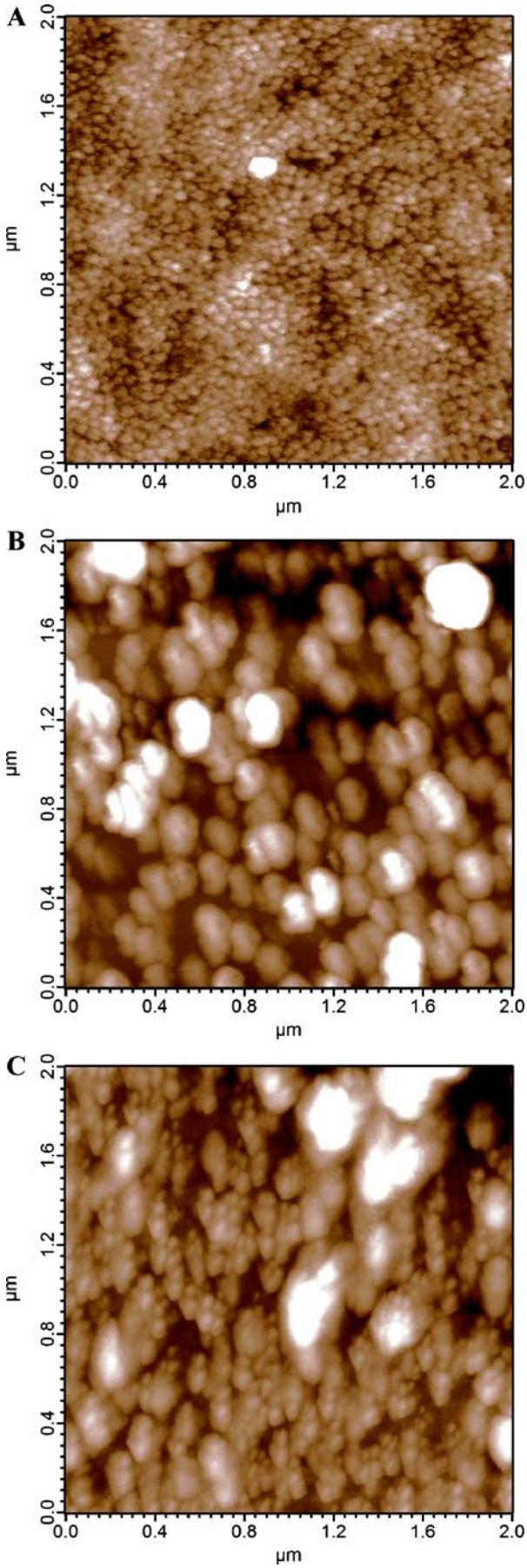

Fig. 6. AFM of uncoated BSA NPs (**A**) obtained right after the coacervation process (i.e., without dialysis) and BSA NPs coated with 50 μg/mL PLL (**B**) and PEI (**C**). Note the uniformity in size and lack of aggregation from (**A**). Larger NPs (200~300 nm) were evident in the samples coated with PLL and PEI, with significant variations in particle sizes. All the images were 2×2 μm in scale and representative images were shown from a large series of images generated from the AFM.

Toxicity of PLL and PEI Coated BSA NPs

Previous studies with PEI coated BSA NPs indicated the PEI coating to be the primary reason for the toxicity of the particles. We accordingly chose a relatively low concentration of polymers (<100 μg/mL), so as to minimize the previously observed toxicity of the NPs. Furthermore, the previous study used myogenic C2C12 cells for toxicity assessment; while they are particularly good for assessing BMP-2 activity, they are more robust than primary cells that may lead to underestimation of NP toxicity. Therefore, BMSC derived from both rats and humans were used in the present study for NP toxicity. BMSC were also chosen since the intended use of our NPs is to deliver BMP-2 and one of the primary targets of BMPs is stem cells at the bone marrow environment. The results of the toxicity assessment are summarized in Fig. 7. Compared to untreated cells, the uncoated NPs did not provide any detectable toxicity, indicating complete removal of the desolvation agent (acetone) during the dialysis procedure. NPs coated with 10–100 μg/mL polymer (either PEI or PLL) also did not provide any significant toxicity in human BMSC (Fig. 7A). There was a slight toxic effect of the particles on rat BMSC ($p \sim 0.02$; Fig. 7B) compared to untreated cells, and a further slight toxic effect of the coatings (except PEI at 10 and 100 μg/mL) compared to the uncoated BSA particles ($p \sim 0.02$). Taken together, this indicated the rat BMSCs were more sensitive to the particles than the human BMSC, but the reduced concentration of PEI and PLL used for NP coating [as compared to (21)] were still relatively well tolerated by the primary cell. Since we were able to get complete coating of the NPs at such low concentrations (based on zeta-potential measurements), coating of NPs at higher concentrations, which might lead to toxicities, were not deemed necessary.

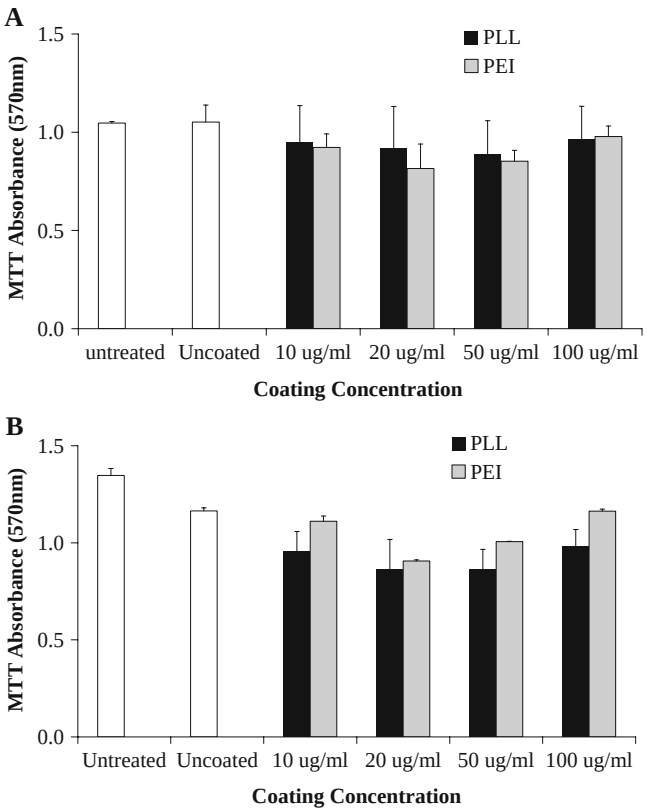

Fig. 7. MTT assay of the PEI and PLL coated NPs in (**A**) human BMSCs and (**B**) rat BMSCs. No significant difference was seen in the toxicity coating concentrations, nor between the different polymer coatings. Data in all graphs were expressed as mean ± SD ($n=3$).

Bioactivity of BMP-2 Encapsulated in Polymer Coated NPs

The NP preparation process was adopted for BMP-2 encapsulation by adding BMP-2 to BSA solution before the coacervation process. The amount of BMP-2 added was only 2.5% of the BSA amount (per weight basis), so that no significant changes in the particle size was observed (as assessed by AFM; not shown), and based on our previous studies, the encapsulation efficiency is supposed to be achieved ~90%. Upregulation of ALP activity is a well-demonstrated feature of BMP-2 induced osteogenic activity on target cells. Several cell types, including myogenic C2C12 cells (21), osteoblastic hBMSC, as well as rBMSC in our hands (22), all display a stimulated ALP induction as a result of BMP-2 treatment. ALP activity is necessary for mineralization, since it is hypothesized to liberate free phosphate in the vicinity of the osteoblast-deposited extracellular matrix and facilitate its calcification. We previously conducted an extensive characterization of rat BMSC after BMP-2 and basic fibroblast Growth Factor (bFGF) treatment, showing lasting effects of BMP-2 on ALP stimulation. We additionally used human BMSC in this study as a more realistic model for clinical application of BMP-2 in bone regeneration. The kinetics and mechanism of BMP-2 release was not addressed in this study due to the difficulties in separating the released BMP-2 and quantitative analysis of such small amount as well as the extensive additional testing that would have required.

Human BMSC were from third passage (P3) in our hands and displayed an ALP activity that was dependent on the passage (Fig. 8A, insert). Cells from passage 4 and 5 displayed BMP-2 induced ALP activity with reduced robustness in the higher passage, and displayed no BMP-2 stimulated ALP activity in passage 6. Therefore, only cells from passage 4 were used for assessment of BMP-2 activity in BSA NPs. hBMSC in all study groups displayed ALP activity that gradually increased over a 14 days period (Fig. 8A). No significant differences were evident among the cells on day 3 for all study groups. Free BMP-2 at 1 μg/mL gave significantly higher ALP activity on day 7 as compared to untreated cells ($p=0.02$). None of the other groups had any significant ALP induction. On day 14, there was no significant ALP activity in cells treated with no BMP-2 (i.e., untreated cells and cells exposed uncoated and polymer-coated NPs in the absence of BMP-2). All BMP-2 containing NPs gave significantly higher ALP activity, and NPs coated with the polymers displayed an equivalent activity to that of free BMP-2. Uncoated NPs with BMP-2 displayed a relatively lower ALP induction. This was likely due to loss of BMP-2 during the processing of the particles since lack of a coating layer was expected to lead to unstable NPs and premature

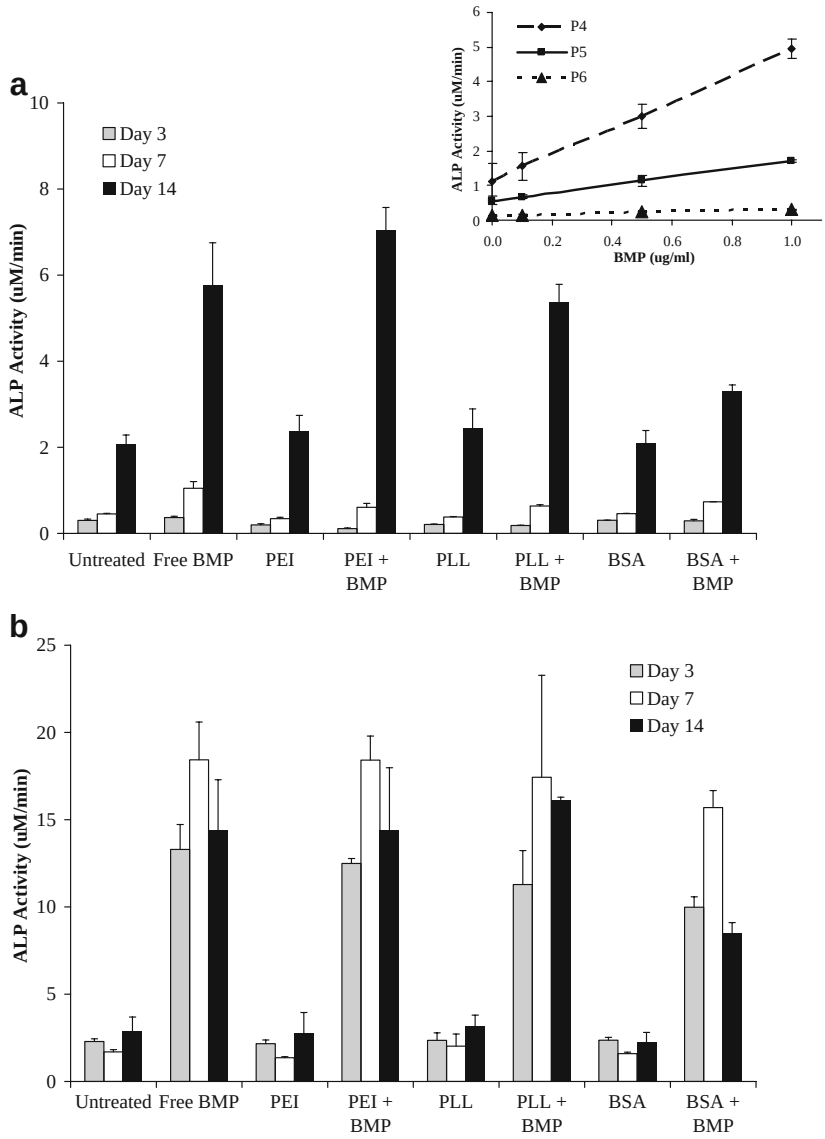

Fig. 8. ALP activity of BMP-2 encapsulated in uncoated and coated NPs in (**A**) human BMSCs and (**B**) rat BMSCs. There was an increase of ALP activity for the NPs containing BMP-2 compared to those without BMP-2 ($p<0.05$). Furthermore the ALP activity for the coated particles were higher than the uncoated ones ($p<0.05$), which was similar to free BMP-2. ALP activity of human BMSCs (*Inset A*) was shown as a function of passage number with the addition of different concentrations of BMP-2. There was a dramatic decrease in ALP activity from passage 4 to passage 6. Data in all graphs were expressed as mean ± SD ($n=3$).

BMP-2 release, but there may also be difficulties in internalizing non-coated particles due to its surface chemistry. Furthermore there was no calcium formation over the 2-week culture period in any of the samples (data not shown).

The ALP activity for the rat BMSC (Fig. 8B) showed a significant increase after day 3 for all samples containing BMP-2 ($p\sim0.01$). Over the entire culture period, the groups not exposed to BMP-2 showed no significant change in ALP activity, however all the groups containing BMP-2 showed a significant increase on day 7. NPs coated with PLL was an exception to this, since the change in ALP activity was not significant between days 3 and 7 due to large SD on day 7. The induced ALP was generally decreased by day 14, though only the uncoated BSA gave a significant decrease ($p\sim0.003$). This decrease in ALP activity was indicative of the cells initiating the mineralization stage of bone formation, which was supported by the calcium assay. The calcium deposition by the rBMSCs was evident at day 14 (Fig. 9) with a significant increase in calcification for all groups containing BMP-2 ($p\sim0.01$). More importantly, the NP encapsulated BMP-2 gave a similar level of calcium deposition as the free BMP-2 at equivalent concentration.

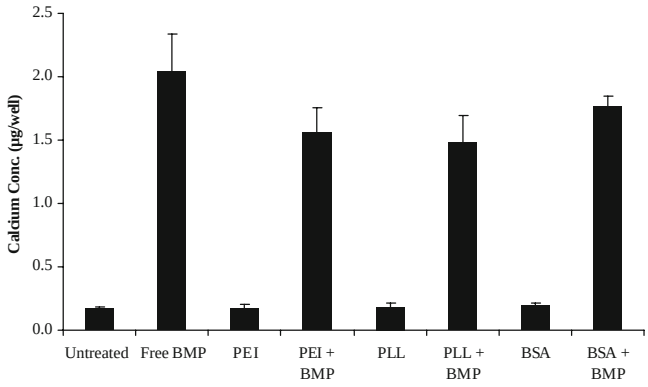

Fig. 9. Calcification of rat BMSCs at day 14. All groups containing BMP-2 showed a significant increase in calcification compared to groups without BMP-2. Data in all graphs were expressed as mean ±

Taken together, the bioactivity results obtained in this study indicated no adverse effect of encapsulation of BMP-2 in NPs. Given the relatively mild entrapment conditions, the use of non-solvent acetone was expected to be the only impediment to retention of BMP-2 activity, and this did not seem to be a concern based on our results. The use of primary cells with direct relevance to osteogenesis provides encouraging data for *in vivo* testing of the proposed formulations. It must be noted that the exact concentration of BMP-2 in NPs were not determined in this study. Based on our previous studies (21), which indicated >90% encapsulation efficiency, we assumed full retention of BMP-2 amount in NPs and tested our formulations against an equivalent concentration of free BMP-2. More detailed studies on factors affecting BMP-2 encapsulation efficiency, BMP-2 release from the NPs, and their consequences on BMP-2 induced osteogenesis will be the subject of future studies.

Other Particulate Delivery Systems for BMP-2

A number of other particulate systems for delivery of BMP-2 have been investigated, including particles prepared from synthetic materials and natural polymers. Among them, hydrolytically degraded polylactic-*co*-glycolic acid (PLGA) are the most investigated delivery system for BMP-2. *In vitro* studies have shown the bioactivity of BMP-2 was maintained during encapsulation into such microparticles (250–430 µm), despite exposure to organic solvents (32). The PLGA particles were effective in stimulating bone formation in several animal models, such as in rat femurs (33), calvarial defects in rabbits (34), and ovine vertebral bodies (35). While some of these studies measured growth factor release, subsequent studies focused on controlling the BMP-2 release from the PLGA particles by embedding them in a calcium phosphate cement (36) or by surface-grafting heparin to the particles for BMP-2 binding (37). These studies utilized particles in the micron-scale, which are not suitable for systemic administration. Only one other system reported PLGA particles with size similar to our particles (~300 nm). This study focused on preventing the rapid diffusion of particles and growth factors away from the implant site by immobilizing PLGA NPs on the surface of a poly(L-lactide) scaffold (38). In addition to synthetic PLGA-based particles, naturally-occurring polymers collagen (39) and dextran (40–42) were also used for BMP-2 entrapment. The particle sizes were again in the micron-scale for these systems (600–700 µm for collagen and 20–40 µm for dextran). Preclinical studies in a rabbit femur (39) and a canine periodontal defect model (40) demonstrated the bioactivity of the BMP-2 *in vivo*. All of the aforementioned delivery systems were designed for local delivery of BMP to a defect site. However, none would be suitable for systemic delivery, since particles <200 nm are ideal for systemic administration. To that extent our protein-based NPs, to the best of our knowledge, provide a unique systemic delivery system for BMP-2, with the ultimate goal of including a bone targeting mechanism. BSA will not be suitable for human clinical application, but this protein can be readily replaced with human serum albumin with little modification of process parameters for NP preparation (2).

CONCLUSIONS

This study demonstrated a reproducible coacervation procedure for preparation of BSA NPs with controllable particle size between 50 and 400 nm. The influences of several process parameters on the size and polydispersity of the NPs were investigated by independent experiments and a statistical methodology. The process variables found to most significantly influence the NP sizes were pH value of the coacervation medium, as well as the concentration of the polymers used for coating the particles. Although initial particle size could be tailored within sub-100 nm range, polymer coating of the particles resulted in an increase of size to ~200 nm range. Smaller particles are more desirable for in vivo administration, since they are less likely to get opsonized and more likely to get extravasated from the circulation. Polymers capable of forming brush-like structures on NP surfaces might be more desirable in this respect, since they might reduce van der Waals based interactions among the NPs, thereby stabilizing them. Nevertheless, the process described successfully entrapped the BMP-2 with significant retention of the bioactivity of the protein, based on *in vitro* bioassays using clinically relevant cell models. We conclude that the NPs described in this study has potential for novel means of BMP-2 delivery, which might further facilitate the clinical application of this protein in local and systemic regeneration of bone tissue.

ACKNOWLEDGEMENTS

The authors thank Xiaoyue Lin and Cezary Kucharski (Faculty of Engineering, University of Alberta) for technical help with cell culture studies. This project was financially supported by an operating grant from the Canadian Institutes of Health Research (CIHR). Guilin Wang is financially supported by a scholarship from the China Scholarship Council. Kevin Siggers is financially supported by a graduate studentship from the Natural Sciences and Engineering Research Council of Canada and a CIHR Team Grant (PI: Derrick Rancourt). BMP-2 was kindly provided by Dr. Walter Sehald (University of Würzburg, Germany)

REFERENCES

1. V. Luginbuehl, L. Meinel, H. P. Merkle, and B. Gander. Localized delivery of growth factors for bone repair. *Euro. J. Pharm. Biopharm.* **58**:197–208 (2004). doi:10.1016/j.ejpb.2004. 03.004.
2. K. Langer, S. Balthasar, V. Vogel, N. Dinauer, H. von Briesen, and D. Schubert. Optimization of the preparation process for human serum albumin (HSA) nanoparticles. *Int. J. Pharm.* **257**:169–180 (2003). doi:10.1016/S0378-5173(03)00134-0.
3. B. G. Muller, H. Leuenberger, and T. Kissel. Albumin nanospheres as carriers for passive drug targeting: an optimized manufacturing technique. *Pharm. Res*. **13**:32–37 (1996). doi:10.1023/A:1016064930502.
4. M. Roser, D. Fischer, and T. Kissel. Surface-modified biodegradable albumin nano- and microspheres. II: effect of surface charges on *in vitro* phagocytosis and biodistribution in rats. *Euro. J. Pharm. Biopharm.* **46**:255–263 (1998). doi:10.1016/S0939-6411(98)00038-1.
5. S. M. Moghimi, A. C. Hunter, and J. C. Murray. Long-circulating and target-specific nanoparticles: theory to practice. *Pharmacol. Rev.* **53**:283–318 (2001).
6. D. C. Litzinger, A. M. J. Buiting, N. van Rooijen, and L. Huang. Effect of liposome size on the circulation time and intraorgan distribution of amphipathic poly(ethylene glycol)-containing liposomes. *Biochim. Biophys. Acta.* **1190**:99–107 (1994). doi:10.1016/0005-2736(94)90038-8.
7. T. O. Harasym, M. B. Bally, and P. Tardi. Clearance properties of liposomes involving conjugated proteins for targeting. *Adv. Drug Deliv. Rev.* **32**:99–118 (1998). doi:10.1016/S0169-409X(97)00134-8.
8. D. V. Devine, and A. J. Bradley. The complement system in liposome clearance: Can complement deposition be inhibited? *Adv. Drug Deliv. Rev.* **32**:19–29 (1998). doi:10.1016/S0169-409X(97)00129-4.
9. D. Thassu, M. Deleers, and Y. Pathak. *Nanoparticulate drug delivery systems*. Informa Healthcare, New York, 2007.
10. C. Plank, K. Mechtler, F. C. Szoka, and E. Wagner. Activation of the complement system by synthetic DNA complexes: a potential barrier for intravenous gene delivery. *Hum. Gene Ther.* **7**:1437–1446 (1996). doi:10.1089/hum.1996.7.12-1437.
11. O. P. Rubino, R. Kowalsky, and J. Swarbrick. Albumin microspheres as a drug delivery system: relation among turbidity ratio, degree of cross-linking, and drug release. *Pharm. Res.* **10**:1059–1065 (1993). doi:10.1023/A:1018979126326.
12. A. B. MacAdam, Z. B. Shafi, S. L. James, C. Marriott, and G. P. Martin. Preparation of hydrophobic and hydrophilic albumin microspheres and determination of surface carboxylic acid and amino residues. *Int. J. Pharm.* **151**:47–55 (1997). doi:10.1016/S0378-5173(97)04886-2.
13. C. Weber, C. Coester, J. Kreuter, and K. Langer. Desolvation process and surface characterisation of protein nanoparticles. *Int. J. Pharm.* **194**:91–102 (2000) Medline. doi:10.1016/S0378-5173(99)00370-1.
14. W. Lin, A. G. A. Coombes, M. C. Davies, S. S. Davis, and L. Illum. Preparation of sub-100 nm human serum albumin nanoparticles using a pH-coacervation method. *J. Drug Target.* **1**:237–243 (1993). doi:10.3109/10611869308996081.
15. M. Rahimnejad, M. Jahanshahi, and G. D. Najafpour. Production of biological nanoparticles from bovine serum albumin for drug delivery. *Afr. J. Biotechnol.* **5**:1918–1923 (2006).
16. J. P. van Miller, S. J. Hermansky, P. E. Losco, and B. Ballantyne. Chronic toxicity and oncogenicity study with glutaraldehyde dosed in the drinking water of Fischer 344 rats. *Toxicology.* **175**:177–189 (2002). doi:10.1016/S0300-483X(02)00080-X.
17. D. McGregor, H. Bolt, V. Cogliano, and H. B. Richter-Reichhelm. Formaldehyde and glutaraldehyde and nasal cytotoxicity: case study within the context of the 2006 IPCS human framework for the analysis of a cancer mode of action for humans. *Crit. Rev. Toxicol.* **36**:821–835 (2006). doi:10.1080/10408440600977669.
18. S. Segura, C. Gamazo, J. M. Irache, and S. Espuelas. Gamma interferon loaded onto albumin nanoparticles: *in vitro* and *in vivo* activities against brucella abortus. *Antimicrob. Agents. Chemother.* **51**:1310–1314 (2007). doi:10.1128/AAC.00890-06.
19. S. Segura, S. Espuelas, M. J. Renedo, and J. M. Irache. Potential of albumin nanoparticles as carriers for interferon gamma. *Drug Dev. Ind. Pharm.* **31**:271–280 (2005).
20. E. Leo, M. Angela Vandelli, R. Cameroni, and F. Forni. Doxorubicin-loaded gelatin nanoparticles stabilized by glutaraldehyde: Involvement of the drug in the cross-linking process. *Int. J. Pharm.* **155**:75–82 (1997). doi:10.1016/S0378-5173(97)00149-X.
21. S. Zhang, G. Wang, X. Lin, M. Chatzinikolaidou, H. Jennissen, H. Uludag. Polyethylenimine-coated albumin nanopartices for BMP-2 delivery. *Biotechnol Prog*. In Press (2008).
22. M. Varkey, C. Kucharski, T. Haque, W. Sebald, and H. Uludag. *In vitro* osteogenic response of rat bone marrow cells to bFGF and BMP-2 treatments. *Clin. Orthop. Relat. Res.* **443**:113–123 (2006). doi:10.1097/01.blo.0000200236.84189.87.
23. S. Zhang, J. E. I. Wright, H. Uludag, and N. Ozber. The interaction of cationic polymers and their bisphosphonate derivatives with hydroxyapatite. *Macromol. Biosci.* **7**:656–670 (2007). doi:10.1002/mabi.200600286.
24. C. Jeney, O. Dobay, A. Lengyel, E. Adam, and I. Nasz. Taguchi optimisation of ELISA procedures. *J. Immunol. Methods.* **223**:137–146 (1999). doi:10.1016/S0022-1759(98)00185-9.
25. C. C. Hung, and H. C. Shih. Experimental design method applied to microwave plasma enhanced chemical vapor deposition diamond films. *J. Crystal Growth.* **233**:723–729 (2001). doi:10.1016/S0022-0248(01)01607-4.
26. H. Jiang, C. Secretan, T. Gao, K. Bagnall, G. Korbutt, J. Lakey, and N. M. Jomha. The development of osteoblasts from stem cells to supplement fusion of the spine during surgery for AIS. *Stud. Health Tech. Informat.* **123**:467–472 (2006).
27. J. Kreuter. Nanoparticles and nanocapsules–new dosage forms in the nanometer size range. *Pharm. Acta Helv.* **53**:33–39 (1978).
28. J. S. Jacob, and E. Mathiowitz. A novel nechanism for spontaneous encapsulation of active agents: phase inversion nanoencapsulation. In S. Svenson (ed.), *Carrier-Based Drug Delivery*, American Chemical Society, Washington, DC, 2004, pp. 214–223.
29. T. Merdan, J. Callahan, H. Petersen, K. Kunath, U. Bakowsky, P. Kopeckova, T. Kissel, and J. Kopecek. Pegylated polyethylenimine-Fab' antibody fragment conjugates for targeted gene delivery to human ovarian carcinoma cells. *Bioconjugate Chem.* **14**:989–996 (2003). doi:10.1021/bc0340767.
30. S. Faraasen, J. Voros, G. Csucs, M. Textor, H. P. Merkle, and E. Walter. Ligand-specific targeting of microspheres to phagocytes by surface modification with poly(L-lysine)-grafted poly(ethylene glycol) conjugate. *Pharm. Res.* **20**:237–246 (2003). doi:10.1023/A:1022366921298.
31. P. C. Hiemenz, and R. Rajagopalan. *Principles of Colloid and Surface Chemistry.* Marcel Dekker, New York, 1997.
32. J. B. Oldham, L. Lu, B. D. Porter, T. E. Hefferan, D. R. Larson, B. L. Currier, A. G. Mikos, and M. J. Yaszemski. Biological activity of rhBMP-2 released from PLGA microspheres. *J. Biomech. Eng.* **122**:289–292 (2008). doi:10.1115/1.429662.
33. S. C. Lee, M. Shea, M. A. Battle, K. Kozitza, E. Ron, T. Turek, R. G. Schaub, and W. C. Hayes. Healing of large segmental defects in rat femurs is aided by RhBMP-2 in PLGA matrix. *J. Biomed. Mat. Res.* **28**:1149–1156 (1994). doi:10.1002/jbm. 820281005.
34. J. Schrier, B. Fink, J. Rodgers, H. Vasconez, and P. DeLuca. Effect of a freeze-dried CMC/PLGA microsphere matrix of rhBMP-2 on bone healing. *AAPS PharmSciTech.* **2**:73–80 (2001). doi:10.1208/pt020318.
35. F. M. Phillips, A. S. Turner, H. B. Seim III, J. MacLeay, C. A. Toth, A. R. Pierce, and D. L. Wheeler. *In vivo* BMP-7 (OP-1) enhancement of osteoporotic vertebral bodies in an ovine model. *Spine J.* **6**:500–506 (2006). doi:10.1016/j.spinee. 2006.01.014.
36. P. Q. Ruhe, O. C. Boerman, F. G. M. Russel, P. H. M. Spauwen, A. G. Mikos, and J. A. Jansen. Controlled release of rhBMP-2 loaded poly(DL-lactic-co-glycolic acid)/calcium phosphate cement composites *in vivo*. *J. Control. Release.* **106**:162–171 (2005). doi:10.1016/j.jconrel.2005.04.018.
37. O. Jeon, S. J. Song, H. S. Yang, S. H. Bhang, S. W. Kang, M. A. Sung, J. H. Lee, and B. S. Kim. Long-term delivery enhances in

vivo osteogenic efficacy of bone morphogenetic protein-2 compared to short-term delivery. *Biochem. Biophys. Res. Commun.* **369**:774–780 (2008). doi:10.1016/j.bbrc. 2008.02.099.

38. G. Wei, Q. Jin, W. V. Giannobile, and P. X. Ma. The enhancement of osteogenesis by nano-fibrous scaffolds incorporating rhBMP-7 nanospheres. *Biomaterials.* **28**:2087–2096 (2007). doi:10.1016/j.biomaterials.2006.12.028.
39. Y. J. Wang, F. H. Lin, J. S. Sun, Y. C. Huang, S. C. Chueh, and F. Y. Hsu. Collagen-hydroxyapatite microspheres as carriers for bone morphogenic protein-4. *Artif.Organs.* **27**:162–168 (2003). doi:10.1046/j.1525-1594.2003.06953.x.
40. F. Chen, Y. Zhao, R. Zhang, T. Jin, H. Sun, Z. Wu, and Y. Jin. Periodontal regeneration using novel glycidyl methacrylated dextran (Dex-GMA)/gelatin scaffolds containing microspheres loaded with bone morphogenetic proteins. *J. Control. Release.* **121**:81–90 (2007). doi:10.1016/j.jconrel.2007.05.023.
41. F. Chen, Z. Wu, Q. Wang, H. Wu, Y. Zhang, X. Nie, and Y. Jin. Preparation of recombinant human bone morphogenetic protein-2 loaded dextran-based microspheres and their characteristics1. *Acta Pharmacol. Sin.* **26**:1093–1103 (2005). doi:10.1111/j.1745-7254.2005.00180.x.
42. F. Chen, Z. Wu, H. Sun, H. Wu, S. Xin, Q. Wang, G. Dong, Z. Ma, S. Huang, Y. Zhang, and Y. Jin. Release of bioactive BMP from dextran-derived microspheres: A novel delivery concept. *Int. J. Pharm.* **307**:23–32 (2006). doi:10.1016/j.ijpharm.2005.09.024.